Characterization of premixed flames in slit geometry: morphology and propagation.

Rachele Lamioni[a,*], Sebastiano Cinnirella[a], Cristiana Bronzoni[b], Marco Folli[b], Leonardo Tognotti[a], Chiara Galletti[a]

[a] *Dipartimento di Ingegneria Civile e Industriale, Università di Pisa, 56126 Pisa, Italy*
[b] *Ricerca & Sviluppo - Laboratorio Sviluppo Prodotti, Immergas S.p.A., Brescello (RE) - Italy*

Abstract

Hydrogen from renewable energy can help decarbonizing domestic heating as hydrogen can be injected directly into the natural gas grid. However, the combustion process in domestic appliances should be studied to evaluate how H2 addition impacts on the end-user performance. In this work, three-dimensional numerical simulations with skeletal kinetic mechanism are carried out to gain insight into the structure of premixed flames issuing from a group of neighbor slits, mimicking a portion of a perforated burner encountered in the domestic condensing boiler. Different flow structures may arise depending on the flow rate in the range of the operating conditions; at large flow rates, the flames issuing from neighbor slits merge leading to a single conical-shaped flame. The addition of H2 anticipates the flame front and affects the flame morphology, especially at high flow rates.

Keywords:
Laminar premixed flame; slit; multi-slit; condensing boilers; Computational Fluid Dynamics.

1. Introduction

It is well accepted that power-to-gas will play a key role in the decarbonization of the energy scenario by allowing to face the issues related or the storage and transport of energy at the time of excess. In particular, hydrogen can be produced in a very sustainable manner through electrolysis from water employing wind or solar power; then hydrogen acts as an energy vector that may exploit the existing distribution infrastructure. Indeed, it has been estimated that 25 TWh of hydrogen could be blended into the European natural gas network by 2030 and that hydrogen could provide about 18% of the energy required for domestic heating in the EU by 2050 [1].

However, adding hydrogen to natural gas influences fuel properties, leading to new challenges for the safe and efficient operation of existing end-user appliances, such as domestic burners and boilers. Even though maximum hydrogen fractions up to 20% are foreseen for domestic applications, there is little proof of the adequate performances of such systems when adding hydrogen [2].

Domestic condensing boilers are usually equipped with perforated burners that inject a premixed mixture into the combustion chamber by providing enough short-length flames to accommodate in compact volumes [2]. The burner design is mainly based on the manufacturers' experience [3]; however, the upcoming injection of hydrogen in the gas grid asks for a better comprehension of the combustion process in such boilers aimed at providing tools for ensuring optimal combustion performances while limiting the pollutants.

This issue would benefit from mathematical models based on Computational Fluid Dynamics (CFD), even though we have to face the complexity of premixed flames [4, 5], as well as the high computational cost required to model the flow, chemical reactions, and heat exchange in the combustion chamber. As concerned domestic boilers, CFD has been mainly applied to the mixing problem upstream of the burner [6–8] or to simplified geometries. Kedia and Ghoniem [9] carried out 2-dimensional simulations with detailed kinetics to investigate the blow-off of a laminar premixed flame issuing from a multi-hole burner. Jothin et al. [10] and Veetil et al. [11] studied numerically the effect of hole-to-hole distance from a multi-hole burner on laminar premixed propane-air and methane-air, respectively, flames. Hinrichs et al. [12] analyzed numerically a single hole of

*Corresponding author:
Email address: rachele.lamioni@dici.unipi.it (Rachele Lamioni)

a cylindrical perforated burner of a domestic condensing boiler by developing a simplified zone to take into account the presence of the heat exchange.

In all the above investigations, flames issue from circular holes; however, the typical perforated burners are usually equipped also with groups of slits. The morphology of flames issuing from groups of slits has been poorly addressed in literature [13–15], especially at the conditions relevant in domestic boilers. Some interesting works on flames from slits exist, but they mainly concern the acoustic response of such flames [16, 17].

This work is aimed at gaining insight into the structure of flames issuing from multi-slit configurations, emulating portions of real burners fitted in the domestic condensing boiler. Besides. we want also to analyze the effect of hydrogen addition by comparing the G222 gas (23% H_2, 77% CH_4) to the conventional G20 gas (100% CH_4).

2. Numerical model

2.1. Physical model

The conservation equations for mass, momentum, energy, and the transport for the mass fractions of chemical species are resolved in steady-state conditions, as:

$$\nabla \cdot (\rho \mathbf{v}) = 0 \quad (1)$$

$$\nabla \cdot (\rho \mathbf{v}\mathbf{v}) = \nabla p + \nabla \cdot (\bar{\tau}) \quad (2)$$

$$\nabla \cdot (\mathbf{v}(\rho E + p)) = \nabla \cdot (k_{eff} \nabla T) + S_h \quad (3)$$

$$(\rho Y_i) + \nabla \cdot (\rho \mathbf{v} Y_i) = -\rho \mathcal{D}_i \nabla^2 Y_i + R_i \quad (4)$$

where $\mathbf{v}$ is the velocity vector, $\bar{\tau}$ is the stress tensor, S_h is the energy source term, including the contribution of radiation, Y_i is the mass fraction of the i-th chemical species and k_{eff} is the effective thermal conductivity. $\mathcal{D}_i$ is the molecular diffusion coefficient of the i-th chemical species in the mixture. R_i is the net rate of production/consumption of the i-th species due to chemical reaction. In particular, we implemented the KEE-Mech [18] kinetic scheme consisting of 17 chemical species and 58 reversible reactions. Radiation is modeled through the P1 model [19, 20] with the weighted-sum-of-gray-gases model with coefficients from Smith [21] to evaluate the spectral properties of the gas media.

2.2. Computational domain and boundary conditions

The multi-slit geometry is shown in Fig. 1 and consists of two slits having a length L and width $w_s = 0.05L$. The edge-to-edge distance between two neighbour slits is $d_w = 0.16L$. The computational domain for

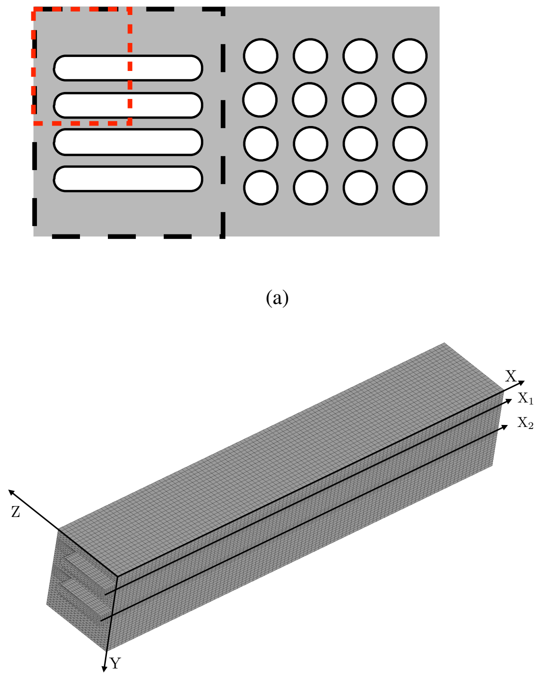

(a)

(b)

Figure 1: Sketch (a) and computational grid (b) of the burner designs.

the configuration comprises two half slits and it is illustrated with a red short-dashed line in Fig. 1a. We noticed how taking advantage of the symmetries, the above domain is representative of a group of 4 slits (black long-dashed line in Fig. 1a) that are encountered in practical burners [3].

The grid is fully structured and was generated by using ICEM by ANSYS Inc., implementing the O-grid strategy to account for the round edges of the slits. Preliminary, we evaluated the thermal flame thickness by performing 1-dimensional simulation of freely propagating flames, with the open-source code Open-Smoke-Suite [22]. Then, the grids were generated to ensure at least 10 nodes within the thermal flame thickness, resulting in 310k computational cells.

2.3. Boundary conditions

Uniform velocity, temperature, and composition were set at the entrance of the slits. To analyze the flame structure, two different velocities in the operating range of domestic condensing boilers, were chosen, i.e. $v_1 = 0.88$ m/s and $v_2 = 2.33$ m/s. The inlet temperature was

$T = 300$ K. The fuel is methane (G20) and methane-hydrogen (G222), the equivalence ratio of the mixture is $\phi = 0.8$. Pressure outlet condition is set at the exit of the domain, while symmetry conditions are prescribed at the sides. As for the wall region between the slits, a wall temperature of $T = 750$ K. Such temperature was selected as it is a common value reported in literature [23–25]. We remark that the above conditions ensure a fully laminar flow.

2.4. Solution methodology

The pressure-based coupled algorithm available in the commercial code FLUENT 19.2 [26] by ANSYS Inc., based on the finite volume method, was used to solve the above governing equations. Discretization was handled by using a central differencing scheme for diffusion terms and a second-order upwind scheme for convection terms. The flame ignition was ensured by patching a region near the inlet with a temperature larger than the adiabatic one, i.e. with $T = 2500$ K. At convergence, the normalized residuals were all below 10^{-6} and did not change with iterations.

3. Results

Figure 2a shows the thermal field for the G20 gas and the lowest inlet velocity, i.e. $v_1 = 0.88$ m/s. To gain a better insight into the 3-dimensional structure of the flame, three longitudinal views are reported, i.e. XY, X_1Z, and X_2Z planes (see Fig. 1b). We can notice how the latter two planes cross the inner and outer slits, respectively. At first glance the temperature distributions on these two planes are similar to each other; the issuing flame appears flat near the axis and subsequently bends towards the edge of the slit. The XY view indicates that the flames do not interact with each other, being well distinct. The only difference is that the flame from the outer slit is slightly tilted because of the different extensions of the adjacent hot walls on its left and right sides.

The structure of the reaction region is visualized through the distribution of OH in Fig. 2b. We can observe that the reaction zone is lifted near the plate external wall, i.e. on the right of the left panel, while it is attached on the left, i.e. towards the inner slits.

The hydrogen addition, i.e., G222 gas, at the lowest velocity, i.e., $v_1 = 0.88$ m/s leads to a flame structure, reported in Fig. 6, which is rather similar to the one described above for the G20 gas. The front of the two flames issuing from the slits remains well distinct. A better insight is provided by the OH profiles along the X_1 and X_2 directions (see Fig. 1b) reported in Fig. 4a for both G20 and G222 gas. We observe slight anticipation of the reaction region with the G222 gas to the G20 one. This can be explained by the fact that the G222 gas contains a limited amount of hydrogen, which represents 23% by volume of the fuel (i.e. 3.6% by weight).

By increasing the inlet velocity to $v_2 = 2.33$ m/s we observe a completely different flame structure. The re-

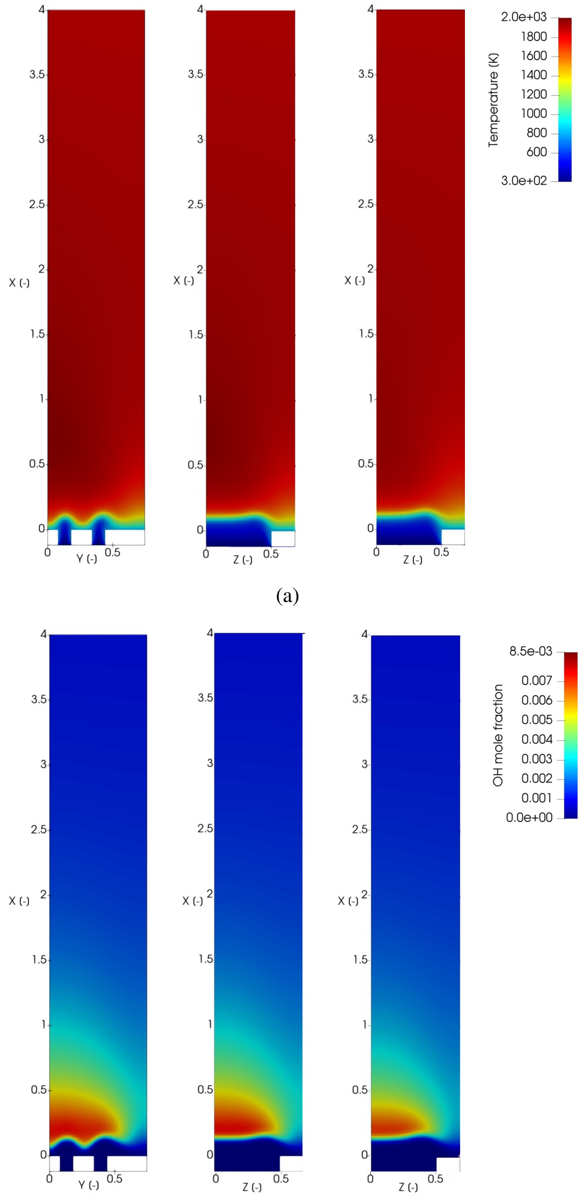

Figure 2: Distribution of (a) temperature and (b) OH mole fraction for G20 gas and v_1 on (from left to right) the XY, X_1Z (i.e., crossing the inner slit) and X_2Z (i.e., crossing the outer slit) planes.

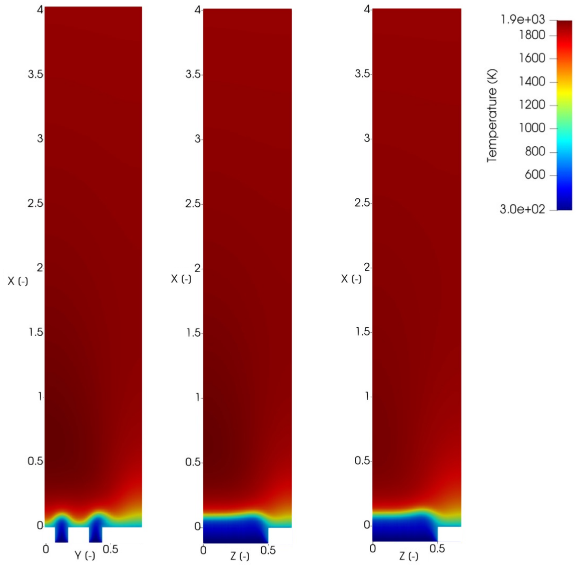

(a)

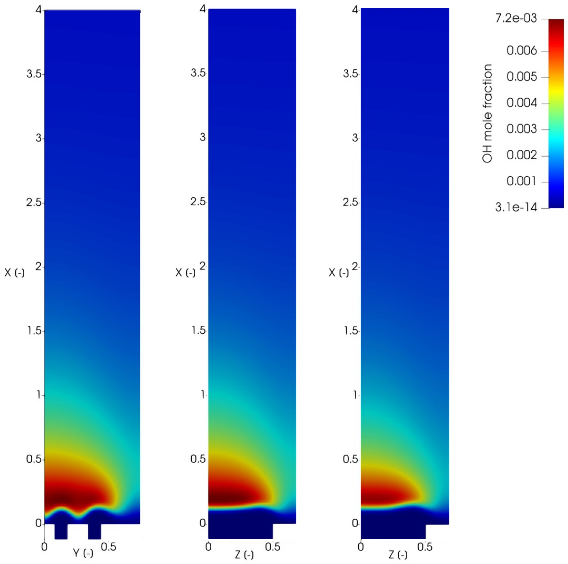

(b)

Figure 3: Distribution of (a) temperature and (b) OH mole fraction for G222 gas and v_1 on (from left to right) the XY, X_1Z (i.e., crossing the inner slit) and X_2Z (i.e., crossing the outer slit) planes. G222 mixture

sults for the G20 gas are shown in Fig. 5. The two flames issuing from the slits are no more separated; instead, they merge leading to a single conical-shaped flame. As a consequence, we can observe that the flames corresponding to the inner and outer slits differ from each other remarkably (see X_1Z and X_2Z planes). In particular, we notice a different penetration of the flames

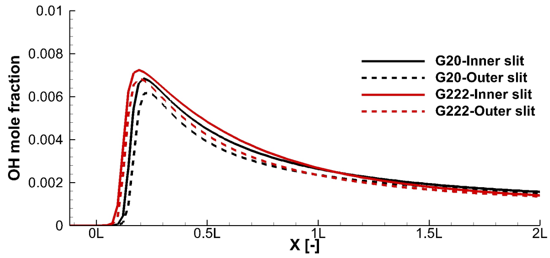

(a)

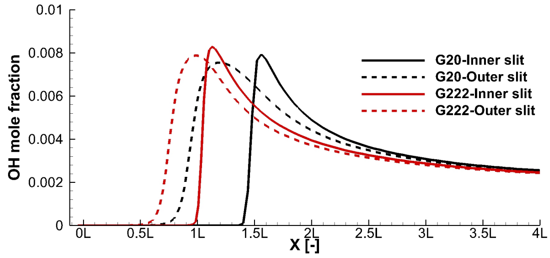

(b)

Figure 4: OH profile along slits axis for (a) v_1 and (b) v_2 for G20 and G222 gases.

from the two slits, with the height of the reaction front of the flame issuing from the outer slit (see right panel of Fig. 5a) being much smaller than that of the inner one. This behavior may be explained by the fact that the flame issuing from the outer slit on the left side encounters strong streams of cold gas (i.e. high-velocity flow from the inner slit), while on the right is affected by the hot burner plate. Hence this flame is anticipated to the flame issuing from the inner slit, which is immersed and surrounded just by cold fresh gases. These differences in the reaction zone are well visible from the OH profiles in Fig. 4b.

Figure 6a shows the results for the highest velocity in case of H_2 addition. Significant differences arise for the G20 gas. Firstly, the flame front appears anticipates, the maximum distance from the burner plate being of $X \approx 1.1L$ for G220 gas, while of $X \approx 1.5L$ for the G20 one. Secondly, also the flame morphology is different. The shape of the flame stemming from the merging of the flames issuing from the slits is no more perfectly conical, but it rather presents a positive curvature near the X axis. The H_2 addition produces an acceleration of the flame front and a different morphology of the flame front. In particular, the flames generated by the inner slit have a greater acceleration than the outer slit. The flame issuing from the outer slit appears closer to the burner, the flame tip being located at $X \approx 0.7L$, than the inner

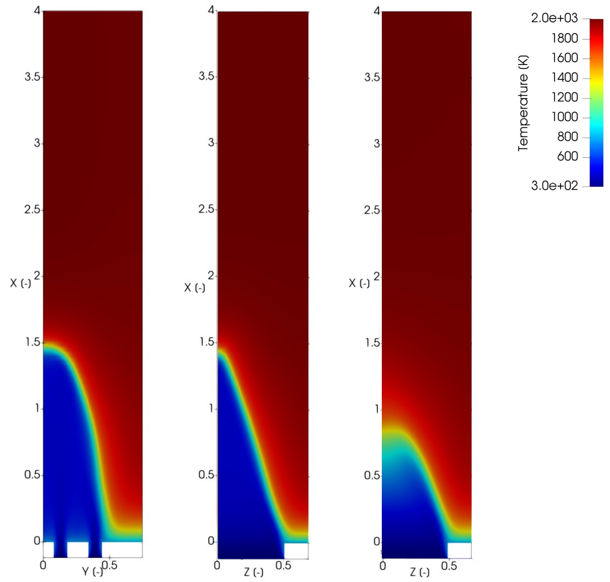

(a)

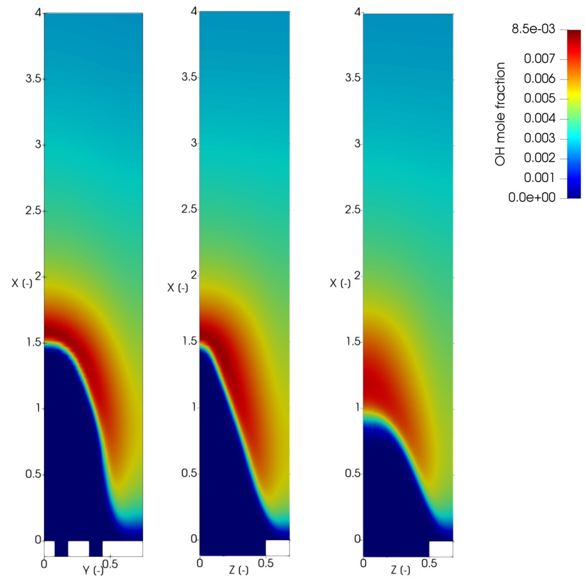

(b)

Figure 5: Distribution of (a) temperature and (b) OH mole fraction for G20 gas and v_2 case on (from left to right) the XY, X_1Z (i.e., crossing the inner slit) and X_2Z (i.e., crossing the outer slit) planes.

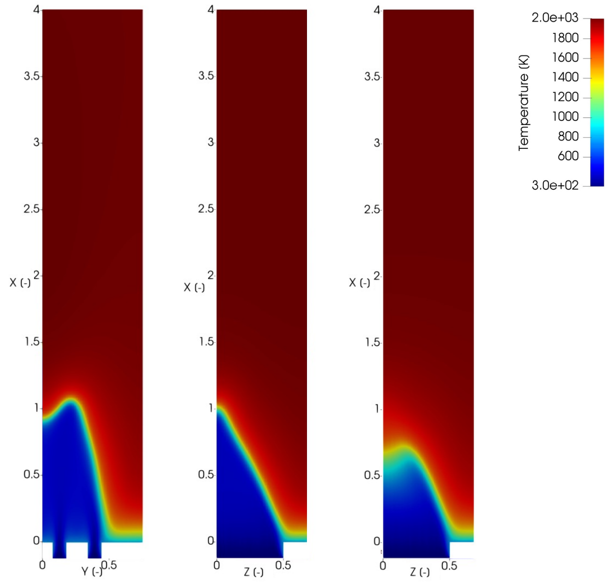

(a)

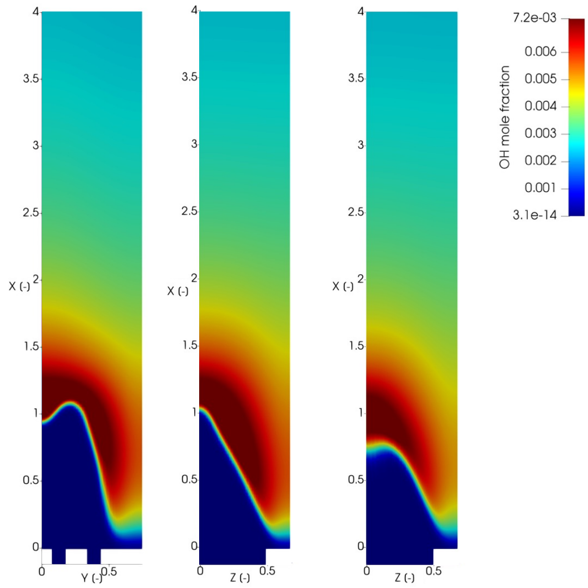

(b)

Figure 6: Distribution of (a) temperature and (b) OH mole fraction for G222 gas and v_2 on (from left to right) the XY, X_1Z (i.e., crossing the inner slit) and X_2Z (i.e., crossing the outer slit) planes.

flame, whose tip is at $X \approx 1L$, as we can see in Fig. 6b, where the OH mole fraction is shown.

4. Conclusions

For low inlet velocities, the flame issuing from a group of slits, emulating a portion of a perforated burner in a domestic condensing boiler, is characterized by the presence of well-separated flames each of them issuing from a slit. Such flames show a flat region along the slit length with a subsequent curvature near its edges. Adding some H_2, i.e. feeding the G222 gas instead of G20 one, leads to slight anticipation of the flame front, even though the flame structure is very similar.

Working at high loads, i.e. increasing the inlet velocity, generates a completely different flame morphology. The flames issuing from neighbor slits merge producing a single conical-shaped flame. As a consequence, the distance of the reaction front from the burner differs remarkably between inner and outer slits. The addition of H_2 strongly anticipates the flame front, despite the limited amount of hydrogen in the G222 mixture. Besides the flame is no more perfectly conical, rather exhibiting a positive curvature near the X axis.

5. Acknowledgments

The present work was supported by the POR FESR 2014-2020 "HyPOWERED" project, funded by Regione Emilia-Romagna Italy.

References

[1] E. Commission, et al., A hydrogen strategy for a climate neutral europe. 2020.

[2] S. Carpentier, P. Milin, N. Mostefaoui, P. Nitschke-Kowsky, J. Schweitzer, Negar Sadegh, O. Thibaut, Self-regulated gas boilers able to cope with gas quality variation state of the art and performances, Report (2018).

[3] F. Schiro, A. Stoppato, Experimental investigation of emissions and flame stability for steel and metal fiber cylindrical premixed burners, Combustion Science and Technology 191 (3) (2019) 453–471.

[4] R. Lamioni, P. E. Lapenna, L. Berger, K. Kleinheinz, A. Attili, H. Pitsch, F. Creta, Pressure-induced hydrodynamic instability in premixed methane-air slot flames, Combustion Science and Technology 192 (11) (2020) 1998–2009.

[5] A. Attili, R. Lamioni, L. Berger, K. Kleinheinz, P. E. Lapenna, H. Pitsch, F. Creta, The effect of pressure on the hydrodynamic stability limit of premixed flames, Proceedings of the Combustion Institute (2020).

[6] T.-H. Zhang, F.-G. Liu, X.-Y. You, Optimization of gas mixing system of premixed burner based on cfd analysis, Energy conversion and management 85 (2014) 131–139.

[7] D.-F. Zhao, F.-G. Liu, X.-Y. You, R. Zhang, B.-L. Zhang, G.-L. He, Optimization of a premixed cylindrical burner for low pollutant emission, Energy Conversion and Management 99 (2015) 151–160.

[8] M. H. Saberi Moghaddam, M. Saei Moghaddam, M. Khorramdel, Numerical study of geometric parameters effecting temperature and thermal efficiency in a premix multi-hole flat flame burner, Energy 125 (2017) 654–662.

[9] K. S. Kedia, A. F. Ghoniem, Mechanisms of stabilization and blowoff of a premixed flame downstream of a heat-conducting perforated plate, Combustion and Flame 159 (3) (2012) 1055–1069.

[10] E. V. Jithin, V. R. Kishore, R. J. Varghese, Three-dimensional simulations of steady perforated-plate stabilized propane-air premixed flames, Energy and Fuels 28 (8) (2014) 5415–5425.

[11] J. Edacheri Veetil, B. Aravind, A. Mohammad, S. Kumar, R. K. Velamati, Effect of hole pattern on the structure of small scale perorated plate burner flames, Fuel 216 (2018) 722–733.

[12] J. Hinrichs, D. Felsmann, S. Schweitzer-De Bortoli, H.-J. Tomczak, H. Pitsch, Numerical and experimental investigation of pollutant formation and emissions in a full-scale cylindrical heating unit of a condensing gas boiler, Applied Energy 229 (2018) 977–989.

[13] R. M. Mallens, B. O. Loijenga, L. P. De Goey, P. J. Sonnemans, Numerical and experimental study of lean M-and V-shaped flames, Combustion Science and Technology 122 (1-6) (1997) 331–344.

[14] R. Mallens, L. P. De Goey, Flash-back of Laminar Premixed Methane/Air Flames on Slit and Tube Burners, Combustion Science and Technology 136 (1-6) (1998) 41–54.

[15] S. Parmentier, M. Braack, U. Riedel, J. Warnatz, Modeling of combustion in a lamella burner, Combustion Science and Technology 175 (1) (2003) 185–206.

[16] V. N. Kornilov, R. Rook, J. H. ten Thije Boonkkamp, L. P. de Goey, Experimental and numerical investigation of the acoustic response of multi-slit Bunsen burners, Combustion and Flame 156 (10) (2009) 1957–1970.

[17] T. Steinbacher, A. Albayrak, A. Ghani, W. Polifke, Consequences of flame geometry for the acoustic response of premixed flames, Combustion and Flame 199 (2019) 411–428.

[18] R. Bilger, S. Stårner, R. Kee, On reduced mechanisms for methane-air combustion in nonpremixed flames, Combustion and Flame 80 (2) (1990) 135–149.

[19] P. Cheng, Two-dimensional radiating gas flow by a moment method, AIAA journal 2 (9) (1964) 1662–1664.

[20] R. Siegel, J. R. Howell, Thermal radiation heat transfer, hemisphere pub, Corp., Washing ton DC (1992).

[21] T. Smith, Z. Shen, J. Friedman, Evaluation of coefficients for the weighted sum of gray gases model (1982).

[22] A. Cuoci, A. Frassoldati, T. Faravelli, E. Ranzi, Opensmoke++: An object-oriented framework for the numerical modeling of reactive systems with detailed kinetic mechanisms, Computer Physics Communications 192 (2015) 237–264.

[23] N. Beishuizen, D. Mayer, Conjugate heat transfer simulations of perforated plate burners using flamelet generated manifolds.

[24] Y. Ding, D. Durox, N. Darabiha, T. Schuller, Chemiluminescence of Burner-Stabilized Premixed Laminar Flames, Combustion Science and Technology 191 (1) (2019) 18–42.

[25] H. Soltanian, M. Z. Targhi, H. Pasdarshahri, Chemiluminescence usage in finding optimum operating range of multi-hole burners, Energy 180 (2019) 398–404.

[26] I. Ansys, Cfd, ICEM CFD theory guide, Ansys inc (2015).